A DC GRID-BASED WIND POWER GENERATION SYSTEM FOR MICRO GRID

Sugunakar Mamidala
Assistant Professor
Deportment Of Eee,
Nishitha College Of Engineering And Technology, Hyderabad, India.

V .Saidulu
Assistant Professor,
Deportment Of Eee,
Aar Mahaveer Engineering College, Hyderabad, India.

Abstract: This paper introduces the outline of a dc grid-based wind power generation system in a poultry cultivate. The proposed system permits adaptable operation of numerous parallel-associated wind generators by dispensing with the requirement for voltage and recurrence synchronization. A model prescient control calculation that offers better transient reaction regarding the adjustments in the working conditions is proposed for the control of the inverters. The plan idea is checked through different test situations to exhibit the operational capacity of the proposed micro grid when it works associated with and islanded from the dissemination grid, and the outcomes got are talked about.

Keywords: Wind power generation, dc grid, energy management, model predictive control.

I.INTRODUCTION

POULTRY cultivating is the raising of trained flying creatures, for example, chickens and ducks to farm meat or eggs for nourishment. To guarantee that the poultries stay gainful, the poultry cultivates in Singapore are required to be kept up at an agreeable temperature. Cooling fans, with power evaluations of several kilowatts, are generally introduced to manage the temperature in the ranches [1]– [3]. Other than cooling the ranches, the wind energy delivered by the cooling fans can be tackled utilizing wind turbines (WTs) to decrease the homesteads' request on the grid. The Singapore government is currently advancing this new idea of collecting wind energy from electric ventilation fans in poultry ranches which has been actualized in numerous nations around the globe [4]. The significant contrast between the circumstance in poultry homesteads and regular wind ranches is in the wind speed fluctuation. The changeability of wind speed in wind cultivates straightforwardly relies upon the natural and climate conditions while the wind speed in poultry ranches is for the most part steady as it is produced by consistent speed ventilation fans. In this manner, the generation irregularity issues that influence the unwavering quality of power supply and power adjust are not common in poultry cultivate wind energy systems.

As of late, the exploration consideration on dc grids has been resurging because of mechanical progressions in power gadgets and energy stockpiling gadgets, and increment in the assortment of dc loads and the entrance of dc dispersed energy assets (DERs, for example, sun powered photovoltaics and power modules. Many research chips away at dc micro grids have been directed to encourage the combination of different DERs and energy stockpiling systems. In [5], [6], a dcmicrogrid based wind cultivate design in which each wind energy change unit comprising of a framework converter, a high recurrence transformer and a solitary stage air conditioning/dc converter is proposed. Be that as it may, the proposed engineering builds the system multifaceted nature as three phases of transformation are required. In [7], a dc micro grid based wind cultivate design in which the WTs are bunched into gatherings of four with each gathering associated with a converter is proposed. Be that as it may, with the proposed design, the disappointment of one converter will bring about each of the four WTs of a similar gathering to be out of administration. The exploration works directed in [8]– [10] are centered around the advancement of various disseminated control procedures to arrange the operation of different DERs and energy stockpiling systems in dc micro grids. These examination works mean to beat the test of accomplishing a decentralized control operation utilizing just neighborhood

factors. Be that as it may, the DERs in dc micro grids are unequivocally coupled to each other and there must be a base level of coordination between the DERs and the controllers. In [11], [12], a half breed air conditioning/dc grid design that comprises of both air conditioning and dc systems associated together by a bidirectional converter is proposed. Progressive control calculations are fused to guarantee smooth power exchange between the air conditioner micro grid and the dc micro grid under different working conditions. Be that as it may, disappointment of the bidirectional converter will bring about the confinement of the dc micro grid from the air conditioner microgrid. An option arrangement utilizing a dc grid based conveyance organize where the air conditioner yields of the wind generators (WGs) in a poultry cultivate are corrected to a typical voltage at the dc grid is proposed in this paper. The most huge preferred standpoint of the proposed system is that exclusive the voltage at the dc grid must be controlled for parallel operation of a few WGs without the need to synchronize the voltage, recurrence and stage, accordingly permitting the WGs to be turned ON or OFF whenever without bringing on any disturbances. Many research chips away at outlining the controllers for the control of inverters in a microgrid amid grid-associated and islanded operations is directed in [13]– [15]. A normally received control conspire which is nitty gritty in [13], [14] contains an internal voltage and current circle and an outer power circle to manage the yield voltage and the power stream of the inverters. In [15], a control plot which utilizes isolate controllers for the inverters amid grid-associated and islanded operations is proposed. Despite the fact that there are a considerable measure of research works being led on the advancement of essential control systems for DG units, there are numerous ranges that require promote change and research consideration. These zones incorporate enhancing the power of the controllers to topological and parametric vulnerabilities, and enhancing the transient reaction of the controllers. To build the controller's heartiness against varieties in the working conditions when the micro grid works in the grid-associated or islanded method of operation and also its ability to deal with requirements, a model-based model prescient control (MPC) outline is proposed in this paper for controlling the inverters. As the micro grid is required to work steadily in various working conditions, the organization of MPC for the control of the inverters offers better transient reaction as for the adjustments in the working conditions and guarantees a more strong micro grid operation. There are some exploration chips away at the execution of MPC for the control of inverters. In [16], a limited control set MPC conspire which takes into consideration the control of various converters without the need of extra

Balance systems or inside course control circles is introduced yet the researchwork does not consider parallel operation of power converters. In [17], an examination on the helpfulness of theMPC in the control of parallel-associated inverters is led. The exploration work is, in any case, concentrated for the most part on the control of inverters for uninterruptible power supplies in independent operation. The MPC calculation will work the inverters near their working cutoff points to accomplish a more better execution as thought about than other control techniques which are typically moderate in taking care of imperatives [18], [19]. In this paper, the inverters are controlled to track occasional current and voltage references and the control signals have a restricted working reach. Under such working condition, the MPC calculation is

working near its working breaking points where the limitations will be activated redundantly. In customary practices, the control signals are cut to remain inside the imperatives, consequently the system will work at the problematic point. This outcomes in sub-par execution and builds the unfaltering state misfortune. MPC, despite what might be expected, tends to influence the shut circle system to work close as far as possible and thus creates far superior execution. MPC has likewise been getting expanded research consideration for its applications in energy management of microgrids in light of the fact that it is a multi-input, multi-yield control technique and takes into consideration the execution of control activities that anticipate future occasions, for example, varieties in power generation by discontinuous DERs, energy costs and load requests [20]– [22]. In these exploration works, the management of energy is defined into various multi-target improvement issues and distinctive MPC techniques are proposed to tackle these enhancement issues. The extent of this paper is however centered around the utilization of MPC for the control of inverters. In what takes after, a far reaching answer for the operation of a dc grid based wind power generation system in a microgrid is proposed for a poultry cultivate and the adequacy of

the proposed system is confirmed by reenactment ponders under various working conditions.

II. SYSTEM DESCRIPTION AND MODELING

A. System Description

The general arrangement of the proposed dc grid based wind power generation system for the poultry cultivate is appeared in Fig. 1. The system can work either associated with or islanded from the dispersion grid and comprises of four 10 kW perpetual magnet synchronous generators (PMSGs) which are driven by the variable speed WTs. The PMSG is considered in this paper since it doesn't require a dc excitation system that will build the outline many-sided quality of the control equipment. The three-stage yield of each PMSG is associated with a three-stage converter (i.e., converters A, B, C and D), which works as a rectifier to control the dc yield voltage of each PMSG to the coveted level at the dc grid. The amassed power at the dc grid is upset by two inverters (i.e., inverters 1 and 2) with each evaluated at 40 kW. Rather than utilizing singular inverter at the yield of each WG, the utilization of two inverters between the dc grid and the air conditioner grid is proposed. This engineering limits the need to synchronize the recurrence, voltage and stage, lessens the requirement for various inverters at the generation side, and gives the adaptability to the fitting and play association of WGs to the dc grid. The accessibility of the dc grid will likewise empower the supply of power to dc stacks all the more effectively by lessening another air conditioner/dc change. The coordination of the converters and inverters is accomplished through a concentrated energy management system (EMS). The EMS controls and screens the power dispatch by each WG and the heap power utilization in the microgrid through a concentrated server. To forestall over the top coursing streams between the inverters, the inverter yield voltages of inverters 1 and 2 are managed to a similar voltage. Through the EMS, the yield voltages of inverters 1 and 2 are consistently observed to guarantee that the inverters keep up a similar yield voltages. The concentrated EMS is likewise in charge of different parts of power management, for example, stack anticipating, unit responsibility, monetary dispatch and ideal power stream. Essential data, for example, field estimations from brilliant meters, transformer tap positions and electrical switch status are altogether sent to the concentrated server for preparing through wireline/remote correspondence. Amid typical operation, the two inverters will share the most extreme yield from the PMSGs (i.e., every inverter shares 20 kW). The most extreme power created by each WT is assessed from the ideal wind power Pwt,opt as takes after [23]:

$$P_{\mathrm{wt,opt}} = k_{\mathrm{opt}}(\omega_{r,\mathrm{opt}})^3 \quad (1)$$

$$k_{\mathrm{opt}} = \frac{1}{2} C_{p,\mathrm{opt}} \rho A \left(\frac{R}{\lambda_{\mathrm{opt}}}\right)^3 \quad (2)$$

$$\omega_{r,\mathrm{opt}} = \frac{\lambda_{\mathrm{opt}} v}{R} \quad (3)$$

where kopt is the streamlined steady, ωr,opt is the WT speed for ideal power generation, Cp,opt is the ideal power coefficient of the turbine, ρ is the air thickness, An is the zone cleared by the rotor cutting edges, λopt is the ideal tip speed proportion, v is the

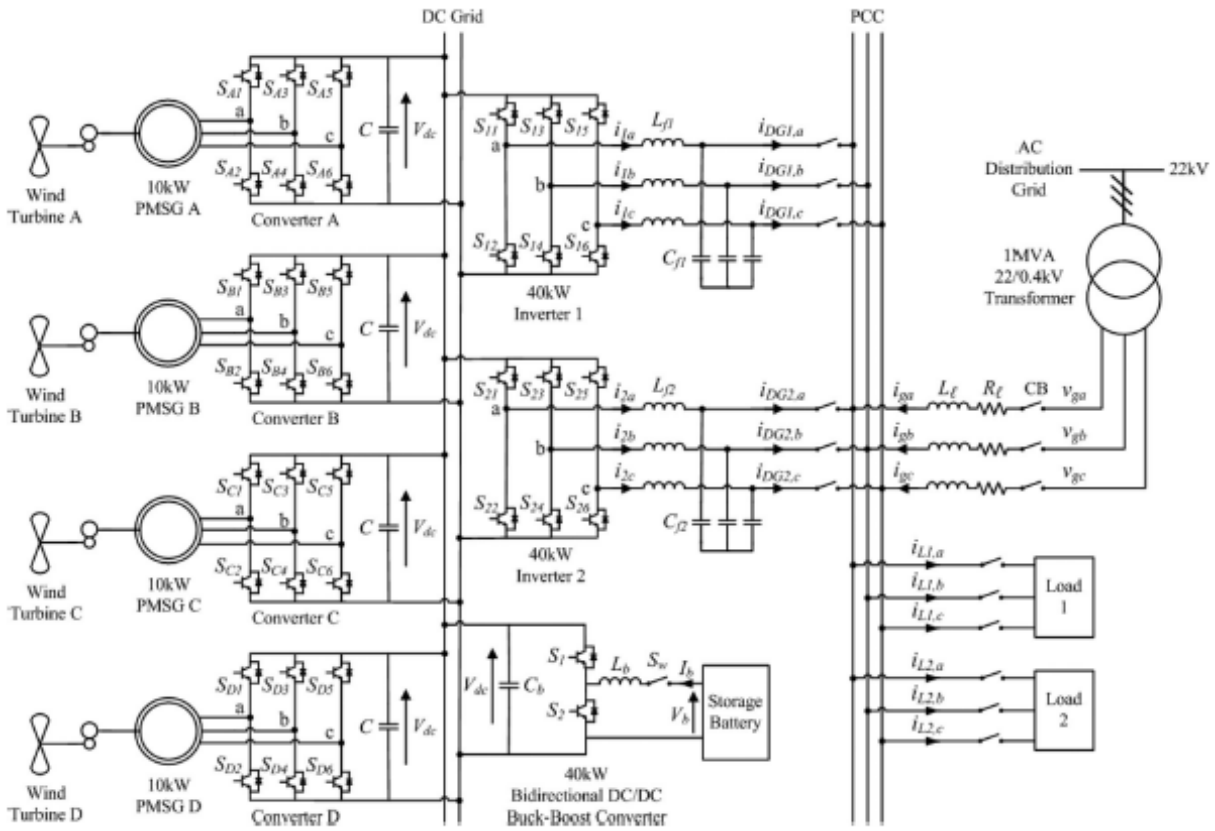

Fig. 1. General arrangement of the proposed dc grid based wind power generation system in a microgrid.

Wind speed and R is the range of the sharp edge. When one inverter neglects to work or is under support, the other inverter can deal with the greatest power yield of 40 kW from the PMSGs. In this way the proposed topology offers expanded unwavering quality and guarantees ceaseless operation of the wind power generation system when either inverter 1 or inverter 2 is separated from operation. A 80 Ah stockpiling battery (SB), which is measured by [24], is associated with the dc grid through a 40 kW bidirectional dc/dc buck-help converter to encourage the charging and releasing operations when the micro grid works associated with or islanded from the grid. The energy requirements of the SB in the proposed dc grid are resolved in light of the system-on-a-chip (SOC) limits given by

$$\mathrm{SOC}_{\min} < \mathrm{SOC} \leq \mathrm{SOC}_{\max} \qquad (4)$$

Despite the fact that the SOC of the SB can't be straightforwardly measured, it can be resolved through the estimation techniques as point by point in [25], [26].With the utilization of a dc grid, the effect of vacillations between power generation and request can be lessened as the SB can quickly come online to direct the voltage at the dc grid. Amid off-crest periods when the power request is low, the SB is energized by the abundance power produced by the WTs. On the other hand, amid top periods when the power request is high, the SB will supplement the generation of the WTs to the heaps.

B. System Operation

At the point when the microgrid is working associated with the circulation grid, the WTs in the microgrid are in charge of giving nearby power support to the heaps, therefore decreasing the weight of power conveyed from the grid. The SB can be controlled to accomplish distinctive request side management capacities, for example, crest shaving and valley filling relying upon the season of-utilization of power and SOC of the SB [27]–[29]. Amid islanded operation where the CBs disengage the micro grid from the circulation grid, the WTs and the SB are just accessible sources to supply the heap request. The SB can supply for the shortage in genuine power to keep up the power adjust of the micro grid as takes after:

$$P_{\mathrm{wt}} + P_{\mathrm{sb}} = P_{\mathrm{loss}} + P_l \qquad (5)$$

where Pwt is the genuine power produced by the WTs, Psb is the genuine power provided by SB which is subjected to the requirement of the SB

greatest power Psb,max that can be conveyed amid releasing and is given by

$$P_{\mathrm{sb}} \leq P_{\mathrm{sb,max}} \qquad (6)$$

Ploss is the system misfortune, and Pl is the genuine power that is provided to the heaps.

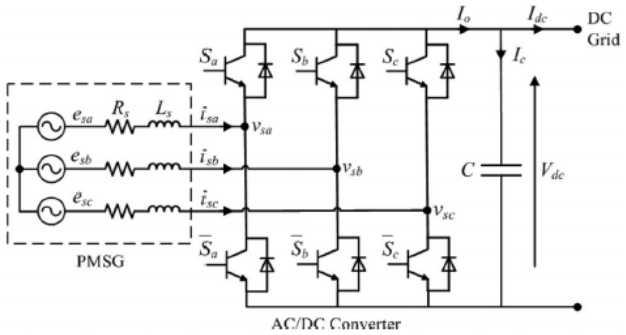

Fig. 2. Power circuit of a PMSG associated with an air conditioner/dc voltage source converter.

C. AC/DC Converter Modeling

Fig. 2 demonstrates the power circuit comprising of a PMSG which is associated with an air conditioner/dc voltage source converter. The PMSG is modeled as an adjusted three-stage air conditioning voltage source esa, esb, esc with arrangement protection Rs and inductance Ls [30], [31]. As appeared in [32], the state conditions for the PMSG streams isa, isb, isc and the dc yield voltage Vdc of the converter can be communicated as takes after:

$$L_s \frac{di_s}{dt} = -R_s i_s + e_s - KSV_{\mathrm{dc}} \qquad (7)$$

$$C\frac{dV_{\mathrm{dc}}}{dt} = i_s^T S - I_{\mathrm{dc}} \qquad (8)$$

where

$$i_s = \begin{bmatrix} i_{\mathrm{sa}} & i_{\mathrm{sb}} & i_{\mathrm{sc}} \end{bmatrix}^T,\ e_s = \begin{bmatrix} e_{\mathrm{sa}} & e_{\mathrm{sb}} & e_{\mathrm{sc}} \end{bmatrix}^T$$

$$K = \begin{bmatrix} 2/3 & -1/3 & -1/3 \\ -1/3 & 2/3 & -1/3 \\ -1/3 & -1/3 & 2/3 \end{bmatrix}$$

$S = \begin{bmatrix} S_a & S_b & S_c \end{bmatrix}^T$ is the ac/dc converter switching functions which are defined as

$$S_j = \begin{cases} 1, & S_j \text{ is ON} \\ 0, & S_j \text{ is OFF} \end{cases} \quad \text{for} \quad j = a,\ b,\ c \qquad (9)$$

D. DC/AC Inverter Modeling

The two 40 kW three-stage dc/air conditioning inverters which interface the dc grid to the point of regular coupling (PCC) are indistinguishable, and the single-stage portrayal of the three-stage dc/air conditioning inverter is appeared in Fig. 3. To infer a state-space model for the inverter, Kirchhoff's voltage and current laws are connected to circle I and point x individually, and the accompanying conditions are gotten:

$$L_f \frac{di}{dt} + iR + v_{\mathrm{DG}} = uV_{\mathrm{dc}} \qquad (10)$$

$$i_{\mathrm{DG}} = i - i_{C_f} \qquad (11)$$

where Vdc is the dc grid voltage, u is the control flag, R is the inverter misfortune, Lf and Cf are the inductance and capacitance of the low-pass (LPF) channel separately, iDG is the inverter yield

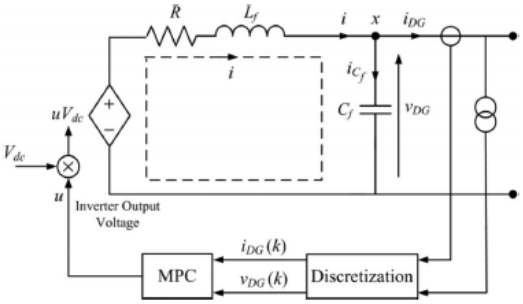

Fig. 3. Single-stage portrayal of the three-stage dc/air conditioning inverter.

current, I is the present coursing through Lf , iCf is the present moving through Cf , and vDG is the inverter yield voltage. Amid grid-associated operation, the inverters are associated with the conveyance grid and are worked in the present control mode (CCM) in light of the fact that the greatness and the recurrence of the yield voltage are attached to the grid voltage. Along these lines, the discrete state-space conditions for the inverter model working in the CCM can be communicated with inspecting time Ts as takes after:

$$x_g(k+1) = A_g x_g(k) + B_{g1} v_g(k) + B_{g2} u_g(k) \qquad (12)$$

$$y_g(k) = C_g x_g(k) + D_g v_g(k) \qquad (13)$$

Where the subscript g speaks to the inverter model amid grid associated operation, k is the ruined present time step, and

$$A_g = 1 - \frac{R}{L_f}T_s,\ B_{g1} = \begin{bmatrix} 0 & -\frac{T_s}{L_f} \end{bmatrix},\ B_{g2} = \frac{V_{\mathrm{dc}}}{L_f}T_s$$

$$C_g = 1,\ D_g = \begin{bmatrix} \frac{C_f}{T_s} & -\frac{C_f}{T_s} \end{bmatrix}$$

xg (k) = i(k) is the state vector; vg (k) = [vDG(k + 1) vDG(k)]T is the exogenous information; ug (k) is the control motion with −1 ≤ ug (k) ≤ 1; and yg (k) = iDG(k) is the yield. The exogenous info vg (k) can be figured utilizing state estimation. In this paper, the grid is set as a substantial power system,which implies that the grid voltage is a steady three-stage sinusoidal voltage. Consequently, while working in the CCM, a three-stage sinusoidal flag can be utilized straightforwardly as the exogenous info. Amid islanded operation, the inverters will be worked in the voltage control mode (VCM). The voltage of

the PCC will be kept up by the inverters when the microgrid is islanded from the grid. When contrasted with Ts , the rate of progress of the inverter yield current is much slower. Hence, the accompanying presumption is made when inferring the state-space conditions for the inverter working in the VCM [33]:

$$\frac{di_{\mathrm{DG}}}{dt} = 0. \qquad (14)$$

In view of the previously mentioned supposition, the discrete state space conditions of the inverter model working in the VCM can

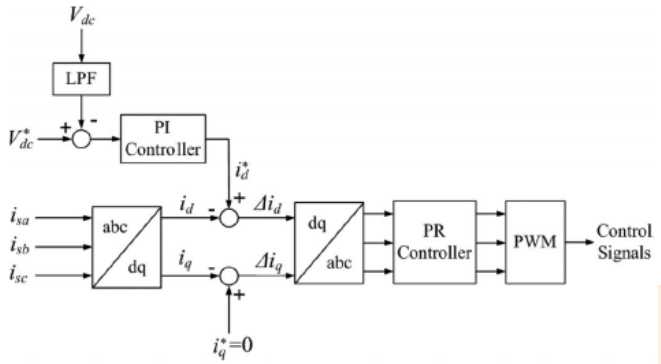

Fig. 4. Arrangement of the proposed controller for the air conditioner/dc converter. Be communicated as takes after:

$$x_i(k+1) = A_i x_i(k) + B_i u_i(k) \qquad (15)$$

$$y_i(k) = C_i x_i(k) \qquad (16)$$

where the subscript I speaks to the model of the inverter amid islanded operation and

$$A_i = \begin{bmatrix} 1 - \frac{R}{L_f}T_s & -\frac{T_s}{L_f} & 0 \\ \frac{T_s}{L_f} & 1 & -\frac{T_s}{C_f} \\ 0 & 0 & 1 \end{bmatrix}, \; B_i = \begin{bmatrix} \frac{V_{\mathrm{dc}}}{L_f}T_s & 0 & 0 \end{bmatrix}$$

$$C_i = \begin{bmatrix} 0 & 1 & 0 \end{bmatrix}$$

xi(*k*) = *i*(*k*) *v*DG(*k*) *i*DG(*k*)

T is the state vector; ui(k) is the control flag with−1 ≤ ui(k) ≤ 1; and yi(k) = vDG(k) is the yield. Amid islanded operation, the inverters are required to convey all the accessible power from the PMSGs to the heaps. In this way, just the inverter yield voltage is controlled and the yield current is resolved from the measure of accessible power.

III. CONTROL DESIGN

A. Control Design for the AC/DC Converter

Fig. 4 demonstrates the design of the proposed controller for every air conditioner/dc voltage source converter which is utilized to keep up the dc yield voltage Vdc of every converter and make up for any variety in Vdc because of any power lopsidedness in the dc grid. The power irregularity will initiate a voltage mistake (V ∗ dc − Vdc) at the dc grid, which is then sustained into a proportionalintegral controller to create a present reference i∗ d for id to track. To dispense with the nearness of high recurrence exchanging swells at the dc grid, Vdc is first gone through a first-arrange LPF. The present iq is controlled to be zero so that the PMSG just conveys genuine power. The present blunders Δid and Δiq are then changed over into the abc casing and nourished into a relative thunderous (PR) controller to create the required control signals utilizing beat width balance.

B. Control Design for the DC/AC Inverter

All together for the microgrid to work in both grid-associated and islanded methods of operation, a model-based controller utilizing MPC is proposed for the control of the inverters. MPC is a model-based controller and embraces a retreating skyline approach in which the improvement calculation will register a grouping of control activities to limit the chose goals for the entire control skyline, yet just execute the principal control activity for the inverter. At whenever step, the streamlining procedure is rehashed in light of new estimations over a moved forecast skyline. Thusly, MPC can influence the yield to track the reference at the following stage, and design and right its control motions along the control procedure. This will ensure a superior transient reaction contrasted with regular PID/PR controllers [32], [33]. To determine the control calculation for the inverters, the state-space conditions are changed into expanded state-space conditions by characterizing the incremental factors in the accompanying organization:

$$\Delta\xi(k) = \xi(k) - \xi(k-1) \qquad (17)$$

where ξ speaks to every factor in the inverter model, for example, vDG, iDG, I and u as appeared in Fig. 3. By characterizing the incremental factors, the expanded state space model for the inverter model working in the CCM amid grid-associated operation can be communicated as takes after:

$$X_g(k+1) = A_{g\_aug}X_g(k) + B_{g1\_aug}V_g(k) + B_{g2\_aug}U_g(k) \quad (18)$$

$$Y_g(k) = C_{g\_aug}X_g(k) \quad (19)$$

where

$$A_{g\_aug} = \begin{bmatrix} 1-\frac{R}{L_f}T_s & 0 \\ 1-\frac{R}{L_f}T_s & 1 \end{bmatrix},$$

$$B_{g1\_aug} = \begin{bmatrix} 0 & 0 & -\frac{T_s}{L_f} \\ -\frac{C_f}{T_s} & \frac{C_f}{T_s} & -\frac{T_s}{L_f} \end{bmatrix}$$

$$B_{g2\_aug} = \begin{bmatrix} \frac{V_{dc}}{L_f}T_s & -\frac{V_{dc}}{L_f}T_s \\ \frac{V_{dc}}{L_f}T_s & -\frac{V_{dc}}{L_f}T_s \end{bmatrix}, \; C_{g\_aug} = [0 \quad 1]$$

$X_g(k) = [\Delta i(k)\ i_{DG}(k)]^T$ is the state vector; $V_g(k) = [\Delta v_{DG}(k+2)\ \Delta v_{DG}(k+1)\ \Delta v_{DG}(k)]^T$ is the exogenous input; $U_g(k) = \Delta u_g(k)$ is the control signal; and $Y_g(k) = i_{DG}(k)$ is the output.

Thus, the expanded state-space model for the inverter model working in the VCM amid islanded operation can be communicated as takes after:

$$X_i(k+1) = A_{i\_aug}X_i(k) + B_{i\_aug}U_i(k) \quad (20)$$

$$Y_i(k) = C_{i\_aug}X_i(k) \quad (21)$$

where

$$A_{i\_aug} = \begin{bmatrix} 1-\frac{R}{L_f}T_s & -\frac{T_s}{L_f} & 0 & 0 \\ \frac{T_s}{L_f} & 1 & -\frac{T_s}{L_f} & 0 \\ 0 & 0 & 1 & 0 \\ \frac{T_s}{L_f} & 1 & \frac{T_s}{L_f} & 1 \end{bmatrix},$$

$$B_{i\_aug} = \begin{bmatrix} \frac{V_{dc}}{L_f}T_s \\ 0 \\ 0 \\ 0 \end{bmatrix}, \; C_{i\_aug} = [0 \quad 0 \quad 0 \quad 1]$$

$X_i(k) = [\Delta i(k)\ \Delta v_{DG}(k)\ \Delta i_{DG}(k)\ v_{DG}(k)]^T$ is the state vector; $U_i(k) = \Delta u_i(k)$ is the control signal; and $Y_i(k) = v_{DG}(k)$ is the output.

For the control of the two enlarged models in the CCM and the VCM, the accompanying cost work is explained utilizing quadratic programming in the proposed MPC calculation [33]:

$$J = (R_s - Y_j)^T(R_s - Y_j) + U_j^T Q U_j \quad (22)$$

subject to the constraint

$$-1 \le u_j(k) \le 1 \quad (23)$$

where Rs is the set-point network, Q is the tuning grid for the coveted shut circle execution, Yj is the yield of either the enlarged model in the CCM or VCM (i.e., Yg or Yi), Uj is the control flag of either the increased model in the CCM or VCM (i.e., Ug or Ui). The initial segment of the cost work is to think about the yield of the enlarged model Yj with the reference Rs and to guarantee that the yield tracks the reference with least blunder. The second piece of the cost work is to compute the weighted factor of the control flag and to guarantee that the control flag produced by theMPC calculation is inside the requirements. The quadratic programming will guarantee that the ideal answer for the control flag deviation Δu is accomplished while limiting the cost work J. After the control flag u is created by the MPC calculation, it will be connected to the dc/air conditioning inverter as appeared in Fig. 3.

IV. NUMERICAL SIMULATION ANALYSIS

The reproduction model of the proposed dc grid based wind power generation system appeared in Fig. 1 is actualized in

TABLE I: PARAMETERS OF THE PROPOSED SYSTEM

Parameter	Value
Distribution grid voltage	$v_g = 230$ V (phase)
DC grid voltage	$V_{dc} = 500$ V
PMSG stator impedance	$R_s = 0.2\ \Omega, L_s = 2.4$ mH
Distribution line impedance	$R_\ell = 7.5\ m\Omega, L_\ell = 25.7\ \mu$H
Inverter LC filter	$L_f = 1.2$ mH, $C_f = 20\ \mu$F
Converter capacitor	$C = 300\ \mu$F
Converter and inverter loss resistance	$R = 1\ m\Omega$
Load 1 rating	$P_{L1} = 35$ kW, $Q_{L1} = 8$ kVAr
Load 2 rating	$P_{L2} = 25$ kW, $Q_{L2} = 4$ kVAr

MATLAB/Simulink. The viability of the proposed plan idea is assessed under various working conditions when the microgrid is working in the grid-associated or islanded method of operation. The system parameters are given in Table I. The impedances of the dispersion line are gotten from [34]. In useful executions, the estimations of the converter and inverter misfortune protection are not definitely known. Consequently, these qualities have been coarsely assessed. A. Experiment 1: Failure of One Inverter During Grid-Connected Operation When the microgrid is working in the grid-associated method of operation, the proposed wind power generation system will supply power to meet piece of the heap request. Under ordinary working condition, the aggregate power produced

by the PMSGs at the dc grid is changed over by inverters 1 and 2 which will share the aggregate power provided to the heaps. When one of the inverters neglects to work and should be disengaged from the dc grid, the other inverter is required to deal with all the power created by the PMSGs. In this experiment, an investigation on the microgrid operation when one of the inverters is separated from operation is directed. With each PMSG producing around 5.5 kWof genuine power, the aggregate power created by the four PMSGs is around 22 kW which is changed over by inverters 1 and 2 into 20 kW and 8 kVAr of genuine and receptive power individually. Figs. 5 and 6 demonstrate the waveforms

of the genuine and receptive power conveyed by inverters 1 and 2 for $0 \leq t < 0.4$ s individually. For $0 \leq t < 0.2$ s, the two inverters 1 and 2 are in operation and every inverter conveys around 10 kW of genuine power and 4 kVAr of receptive power to the heaps. The staying genuine and receptive power that is requested by the heaps is provided by the grid which is appeared in Fig. 7. It can be seen from Fig. 7 that the grid conveys 40 kW of genuine power and 4 kVAr of responsive power to the heaps for $0 \leq t < 0.2$ s. The aggregate genuine and responsive power provided to the heaps is around 60 kW and 12 kVAr as appeared in the power waveforms of Fig. 8. The shaky estimations saw in the power waveforms for $0 \leq t < 0.08$ s are on account of the controller requires a time of around four cycles to track the power references amid the instatement time frame. When contrasted with ordinary control systems, it can be watched that the proposed MPC calculation can rapidly track and settle to the power reference. This is credited to the advancement of the inverters through the

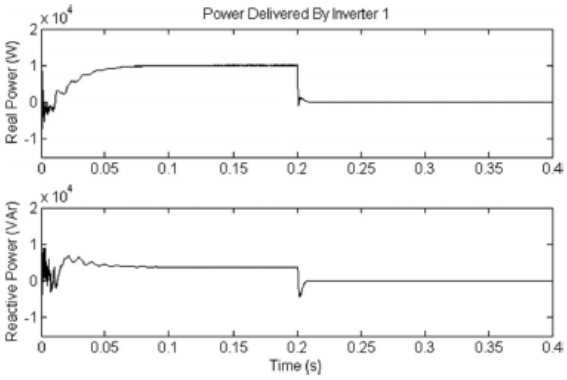

Fig. 5. Real (top) and reactive (bottom) power delivered by inverter 1.

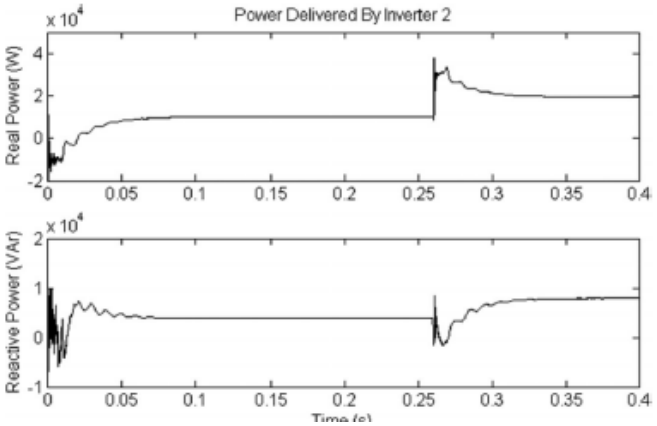

Fig. 6. Real (top) and reactive (bottom) power delivered by inverter 2.

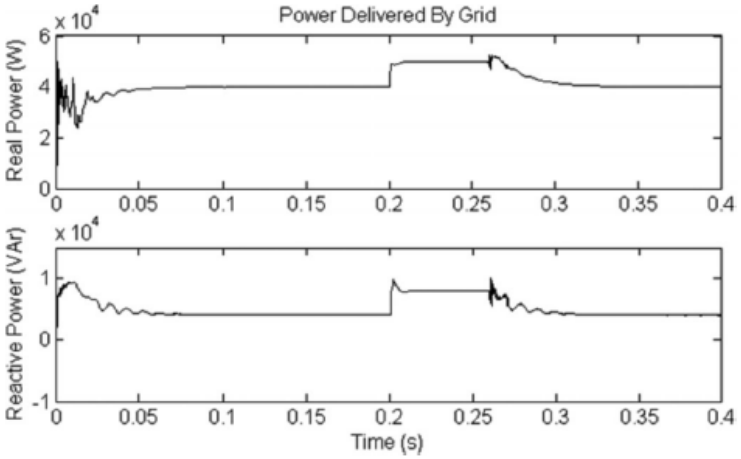

Fig. 7. Real (top) and reactive (bottom) power delivered by the grid.

model-based MPC control. Basically, model-based control plans can consider the system parameters with the end goal that the general execution can be improved. At t = 0.2 s, inverter 1 neglects to work and is disengaged from the microgrid, bringing about lost 10 kW of genuine power and 4 kVAr of responsive power provided to the heaps. As appeared

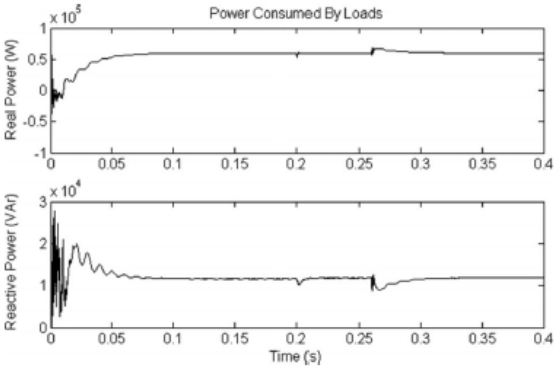

Fig. 8. Real (top) and reactive (bottom) power consumed by the loads.

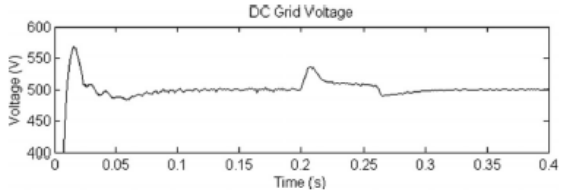

Fig. 9. DC grid voltage.

in Fig. 5, the genuine and responsive power provided by inverter 1 is diminished to zero in about a large portion of a cycle after inverter 1 is detached. This undelivered power causes a sudden power surge in the dc grid which compares to a voltage ascend at t = 0.2 s as appeared in Fig. 9. To guarantee that the heap request is met, the grid naturally expands its genuine and receptive power generation to 50 kW and 8 kVAr individually at t = 0.2 s, as appeared in Fig. 7. At t = 0.26 s, the EMS of the microgrid expands the reference genuine and receptive power provided by inverter 2 to 20 kW and 8 kVAr individually. A deferral of three cycles is acquainted with cook for the reaction time of the EMS to the loss of inverter 1. As appeared in Fig. 6, inverter 2 figures out how to expand its genuine and receptive power provided to the heaps to 20 kW and 8 kVAr for $0.26 \leq t < 0.4$ s. In the meantime, the grid diminishes its genuine and receptive power back to 40 kW and 4 kVAr as appeared in Fig. 7 separately. The power adjust in the microgrid is reestablished after three cycles from t = 0.26 s. It is seen from Fig. 9 that the voltage at the dc grid relates to a voltage plunge at t = 0.26 s because of the expansion in power drawn by inverter 2 and at that point comes back to its ostensible estimation of 500 V for $0.26 \leq t < 0.4$ s. As saw in Fig. 8, at t = 0.26 s, the adjustments in power conveyed by inverter 2 and the grid additionally cause a transient in the heap power. B. Experiment 2: Connection of AC/DC Converter During Grid-Connected Operation The most huge favorable position of the proposed dc grid based wind power generation system is that it encourages the association

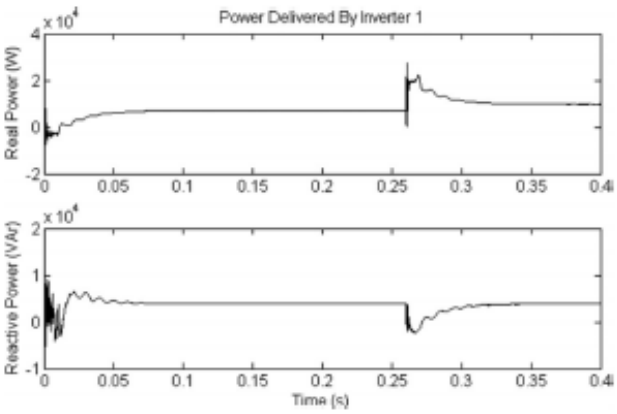

Fig. 10. Real (top) and reactive (bottom) power delivered by inverter 1.

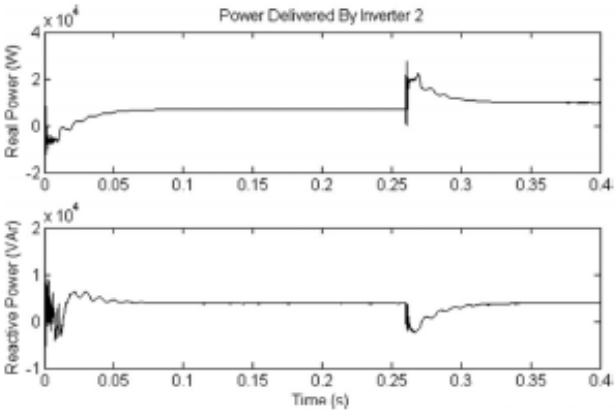

Fig. 11. Real (top) and reactive (bottom) power delivered by inverter 2.

of any PMSGs to the microgrid without the need to synchronize their voltage and recurrence. This ability is shown for this situation consider. The microgrid works associated with the grid and PMSG An is separated from the dc grid for $0 \leq t < 0.2$ s as appeared in Fig. 1. The genuine power created from each of the staying three PMSGs is kept up at 5.5 kW and their accumulated genuine power of 16.5 kW at the dc grid is changed over by inverters 1 and 2 into 14 kW of genuine power and 8 kVAr of responsive power. As appeared in Figs. 10 and 11, every inverter conveys genuine and receptive power of 7 kW and 4 kVAr to the heaps separately. Whatever is left of the genuine and responsive power request of the heaps is provided by the grid as appeared in Fig. 12. It can be seen from Fig. 12 that the grid conveys 46 kWof genuine power and 4 kVAr of responsive power to the heaps. At t = 0.2 s, PMSG A which creates genuine power of 5.5 kW is associated with the dc grid. This causes a sudden power surge at the dc grid and results in a voltage ascend at t = 0.2 s as appeared in the voltage waveform of Fig. 13. At t = 0.26 s, the EMS builds the genuine conveyed by every inverter to 10 kW while the receptive power provided by every inverter stays unaltered at 4 kVAr as

appeared in Figs. 10 and 11. This causes an immediately

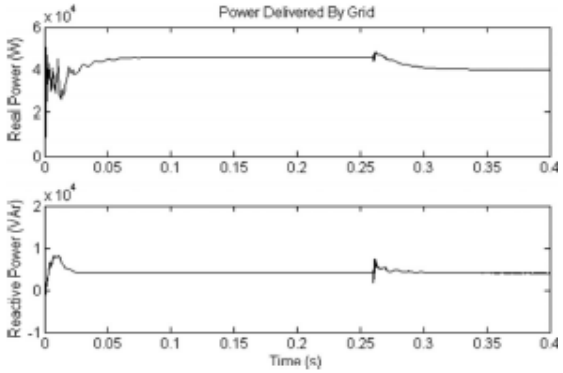

Fig. 12. Real (top) and reactive (bottom) power delivered by the grid.

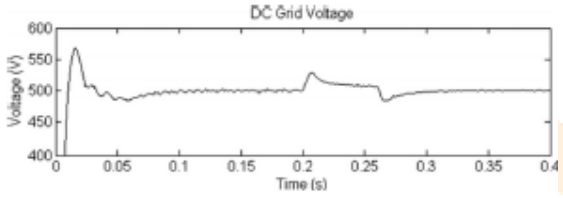

Fig. 13. DC grid voltage.

plunge in the dc grid voltage at t = 0.26 s as saw in Fig. 13 which is then reestablished back to its ostensible voltage of 500 V for $0.26 \leq t < 0.4$ s. The grid likewise at the same time diminishes its supply to 40 kW of genuine power for $0.26 \leq t < 0.4$ s while its receptive power stays steady at 4 kVAr as appeared in Fig. 12. C. Experiment 3: Islanded Operation When the microgrid works islanded from the dissemination grid, the aggregate generation from the PMSGs will be lacking to supply for all the heap request. Under this condition, the SB is required to dispatch the essential power to guarantee that the microgrid keeps on working steadily. The third contextual investigation demonstrates the microgrid operation when it islands from the grid. The microgrid is at first working in the grid-associated mode. The grid is providing genuine power of 40 kW and responsive power of 4 kVAr to the heaps for $0 \leq t < 0.2$ s as appeared in Fig. 14 while every inverter is conveying genuine power of 10 kW and receptive power of 4 kVAr to the heaps as appeared in Figs. 15 and 16. At t = 0.2 s, the microgrid is disengaged from the appropriation grid by the CBs because of a blame happening in the upstream system of the conveyance grid. It can be seen from Fig. 14 that the CBs completely isolate the microgrid from the grid in about a large portion of a cycle, bringing about zero genuine and receptive power provided by the grid for $0.2 \leq t < 0.4$ s.With the loss of power supply from the grid, the power awkwardness between the generation and load request is identified by the EMS. To keep up the soundness of the microgrid, the SB is entrusted by the EMS to

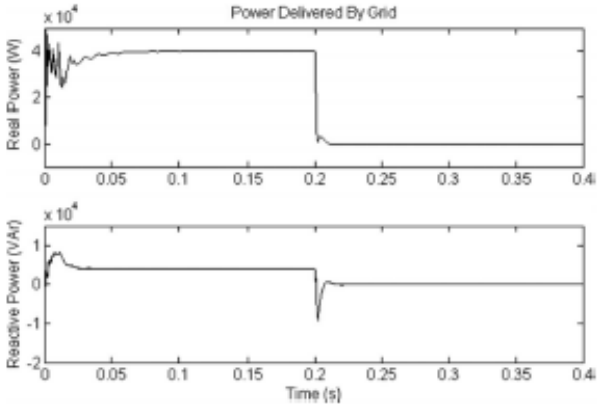

Fig. 14. Real (top) and reactive (bottom) power delivered by the grid.

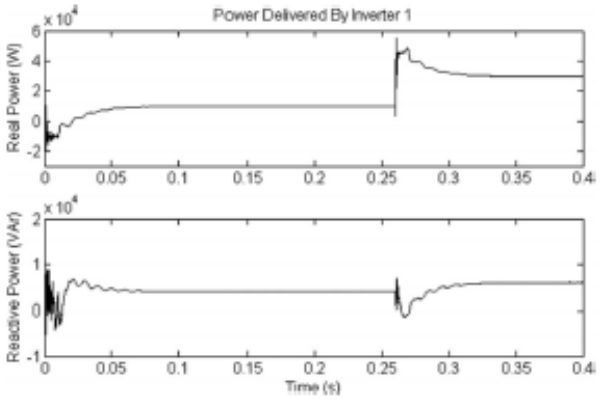

Fig. 15. Real (top) and reactive (bottom) power delivered by inverter 1.

supply genuine power of 40 kW at t = 0.26 s as appeared in Fig. 17. In the meantime, the genuine and receptive power conveyed by every inverter is additionally expanded by the EMS to 30 kW and 6 kVAr as appeared in Figs. 15 and 16 individually. Fig. 18 demonstrates the dc grid voltage where slight voltage changes are seen at t = 0.26 s. The underlying voltage ascend at t = 0.26 s is because of the power provided by the SB while the consequent voltage plunge is because of the expansion in power drawn by the inverters.

V. CONCLUSION

In this paper, the plan of a dc grid based wind power generation system in a microgrid that empowers parallel operation of severalWGs in a poultry cultivate has been introduced. As thought about to regular wind power generation systems, the proposed microgrid engineering disposes of the requirement for voltage and recurrence synchronization, consequently permitting the WGs to be turned on or off with negligible aggravations

to the microgrid operation. The plan idea has been confirmed through different test situations to exhibit the operational ability of the proposed microgrid and the recreation comes about has demonstrated that the proposed outline idea can offer expanded adaptability

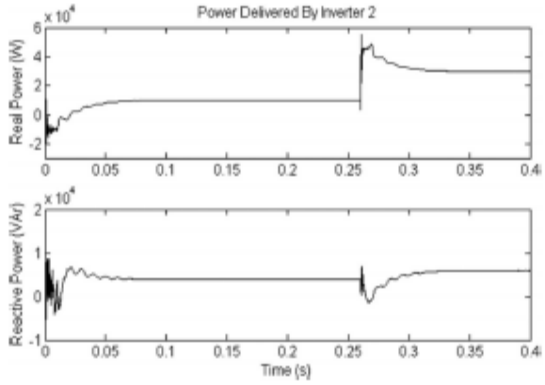

Fig. 16. Real (top) and reactive (bottom) power delivered by inverter 2.

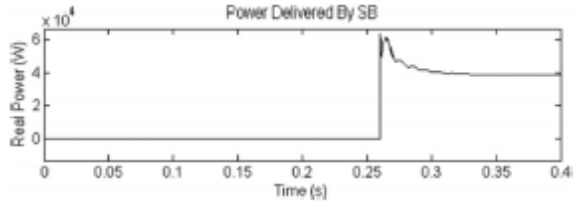

Fig. 17. Real power delivered by SB.

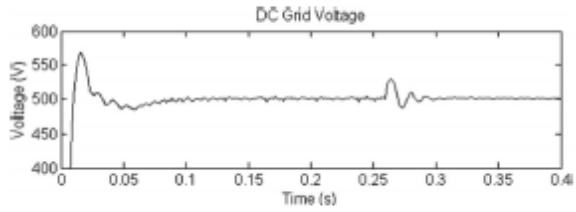

Fig. 18. DC grid voltage.

what's more, dependability to the operation of the microgrid. Nonetheless, the proposed control configuration still requires advance exploratory approval since estimation mistakes because of mistakes of the voltage and current sensors, and modeling blunders because of varieties in genuine system parameters, for example, dissemination line and transformer impedances will influence the execution of the controller in viable usage. Also, MPC depends on the exactness of model foundation, henceforth additionally examine on enhancing the controller vigor to modeling mistake is required. The reenactment comes about got and the investigation performed in this paper fill in as a reason for the plan of a dc grid based wind power generation system in a microgrid.

REFERENCES

1. M. Czarick and J.Worley, “Wind turbines and tunnel fans,” *Poultry Housing Tips*, vol. 22, no. 7, pp. 1–2, Jun. 2010.
2. [Farm Energy: Energy efficient fans for poultry production. [Online].Available:
3. http://farmenergy.exnet.iastate.edu.
4. A. Mogstad, M. Molinas, P. Olsen, and R. Nilsen, “A power conversion system for offshore wind parks,” in Proc. 34th IEEE Ind. Electron., 2008, pp. 2106–2112.
5. A. Mogstad and M. Molinas, “Power collection and integration on the electric grid from offshore wind parks,” in Proc. Nordic Workshop Power Ind. Electron., 2008, pp. 1–8.
6. D. Jovic, “Offshore wind farm with a series multiterminal CSI HVDC,” Elect. Power Syst. Res., vol. 78, no. 4, pp. 747–755, Apr. 2008.
7. X. Lu, J. M. Guerrero, K. Sun, and J. C Vasquez “An improved droop control method for DC microgrids based on low bandwidth communication with DC bus voltage restoration and enhanced current sharing accuracy,” IEEE Trans. Power Electron., vol. 29, no. 4, pp. 1800–1812, Apr. 2014.
8. T. Dragicevi, J. M. Guerrero, and J. C Vasquez, “A distributed control
9. strategy for coordination of an autonomous LVDC microgrid based
10. on power-line signaling,” IEEE Trans. Ind. Electron., vol. 61, no. 7, pp. 3313–3326, Jul. 2014.
11. N. L. Diaz, T. Dragicevi, J. C. Vasquez, and J. M. Guerrero, “Intelligent
12. distributed generation and storage units for DC microgrids—A new concept on cooperative control without communications beyond droop control,” IEEE Trans. Smart Grid, vol. 5, no. 5, pp. 2476–2485,
13. Sep. 2014.
14. X. Liu, P. Wang, and P. C. Loh, “A hybrid AC/DC microgrid and its coordination control,” IEEE Trans. Smart Grid, vol. 2, no. 2, pp. 278–286, Jun. 2011.
15. [C. Jin, P. C. Loh, P. Wang, M. Yang, and F. Blaabjerg, “Autonomous operation of hybrid AC-DC microgrids,” in Proc. IEEE Int. Conf. Sustain. Energy Technol., 2010, pp. 1–7.
16. J. A. P. Lopes, C. L. Moreira, and A. G.Madureira, “Defining control strategies for microgrids islanded operation,” IEEE Trans. Power Syst., vol. 21, no. 2, pp. 916–924, May 2006.

17. Y. Li, D. M. Vilathgamuwa, and P. Loh, "Design, analysis, and real-time testing of a controller for multibus microgrid system," IEEE Trans. Power Electron., vol. 19, no. 5, pp. 1195–1204, Sep. 2004.
18. C. L. Chen, Y. B. Wang, J. S. Lai, Y. S. Lai, and D. Martin, "Design of parallel inverters for smooth mode transfer of microgrid applications," IEEE Trans. Ind. Electron., vol. 25, no. 1, pp. 6–15, Jan. 2010.
19. S. Kouro, P. Cortes, R. Vargas, U. Ammann, and J. Rodr´ıguez, "Model predictive control—A simple and powerful method to control power converters," IEEE Trans. Ind. Electron., vol. 56, no. 6, pp. 1826–1838, Jun. 2009.
20. K. S. Low and R. Cao, "Model predictive control of parallel-connected inverters for uninterruptible power supplies," IEEE Trans. Ind. Electron., vol. 55, no. 8, pp. 2884–2893, Aug. 2008.